Cardiolipin–Cholesterol Interactions in the Liquid-Crystalline Phase: A Steady-State and Time-Resolved Fluorescence Anisotropy Study with *cis*- and *trans*-Parinaric Acids as Probes†

Jacques Gallay* and Michel Vincent

Equipe de Recherche No. 64 du Centre National de la Recherche Scientifique, Unité d'Enseignement et de Recherche Biomédicale des Saints-Pères, 75270 Paris Cedex 06, France

Received August 19, 1985; Revised Manuscript Received December 31, 1985

ABSTRACT: The potency of cholesterol to affect the acyl chain order and dynamics of cardiolipin membranes in the liquid-crystalline state was monitored by steady-state and time-resolved fluorescence anisotropy as well as excited-state lifetime measurements with *cis*- and *trans*-parinaric acids as probes. Up to a cholesterol mole fraction ($\bar{X}_{chl}$) of $\simeq$0.20, no measurable effect on any of the fluorescence parameters of either probe in cardiolipin bilayers was evidenced. This was in striking contrast to the situation in dioleoylphosphatidylcholine (DOPC), for which a cholesterol mole fraction of 0.20 corresponded to the half-maximal effect on the fluorescence parameters, reflecting the classical ordering effect of cholesterol observed in lecithin systems in the liquid-crystalline phase. Whereas in DOPC bilayers this order effect plateaued at $\bar{X}_{chl}$ = 0.50, in cardiolipins the increase in acyl chain order was observable up to a mole fraction as high as 0.80. This indicated that cardiolipins were able to incorporate about 4 mol of cholesterol/mol of cardiolipin (i.e., 1 mol of cholesterol per fatty acyl chain). Besides, ^{31}P NMR spectra of multilamellar liposomes obtained from pure cardiolipins and cardiolipin–cholesterol mixtures evidenced a line shape characteristic of lamellar structures. These results clearly indicate that the presence of high levels of cardiolipins in inner mitochondrial membrane does not impede cholesterol uptake by these membranes. However, the absence of an effect of cholesterol in the physiological range of the cholesterol mole fraction ($\simeq$0.20) would signify weaker sterol–cardiolipin interactions than with lecithins and in turn would explain the relative dearth of cholesterol in these membranes.

The distribution of cholesterol between the different cell membranes has been recognized to be nonuniform in the majority of the investigated tissues in eukaryotes (Brückdorfer & Graham, 1976; Rouser, 1983). A decreasing cholesterol content from plasma membranes to mitochondrial inner membranes has been observed, the other subcellular membranes presenting intermediate values. The mechanisms involved in the control of this cholesterol gradient are not well understood. It has been suggested that cholesterol can exchange from its sites of synthesis in the endoplasmic reticulum membranes to the other cell membranes via cytosolic transport proteins (Chanderbahn et al., 1982). Recently, it has been shown that newly synthesized cholesterol was rapidly transferred to the cell surface probably via membrane vesicles (Lange & Matthies, 1984). Net transfer from lipoproteins to plasma membranes may also occur as in erythrocyte membranes where the cholesterol level is primarily determined by plasma unesterified cholesterol (Lange & d'Alessandro, 1977). In addition to the existence of these shuttle mechanisms, the lipid composition of the different membranes must play a role in maintaining the cholesterol gradient. In this respect, it has been observed, for instance, that PE[1]-rich membranes such as those in bacteria exhibited very low level of sterols (Demel & de Kruijff, 1976) whereas the highest levels were found in PC- and sphingomyelin-rich membranes, i.e., plasma membranes from eukaryotic cells. Low levels of cholesterol have been also found in inner mitochondrial membranes which are rich in PE and in cardiolipins (Brückdorfer & Graham, 1976).

As compared to PE–cholesterol systems for which many data are available (Van Dijck et al., 1976; Demel et al., 1977; Cullis et al., 1978; Blume & Griffin, 1982; Ghosh & Seelig, 1982), little is known about cardiolipin–cholesterol interactions (Boggs & Hsia, 1973). This prompted us to address the question of whether this phospholipid could accommodate cholesterol in the liquid-crystalline phase as PC's and PE's do (Demel & de Kruijff, 1976). Hence, the effect of cholesterol incorporation in cardiolipin vesicles on acyl order and dynamics was monitored by steady-state and time-resolved fluorescence anisotropy with *trans*- and *cis*-parinaric acids as fluorescent probes.

These natural fluorescent fatty acids exhibit only weak perturbations on their microenvironment. Their spectroscopic properties as well as their partition properties have been widely studied (Sklar et al., 1975, 1977 a,b, 1979a,b; Tecoma et al., 1977; Wolber & Hudson, 1981; Welti, 1982; Welti & Silbert, 1982; Pugh et al., 1982; Parassassi et al., 1984). Their excited-state characteristics in what concerns the orientation of the dipole moments with respect to the molecular principal symmetry axis make them useful for anisotropy decay studies

† This work was partially supported by the Institut National de la Santé et de la Recherche Médicale (ex U.221).

* Author to whom correspondence should be addressed.

[1] Abbreviations: CL, cardiolipin (beef heart mitochondrial source); CHL, cholesterol; DOPC, 1,2-dioleoyl-*sn*-glycero-3-phosphocholine; PC, phosphatidylcholine; PE, phosphatidylethanolamine; *cis*-PnA, *cis*,*trans*,*trans*,*cis*-9,11,13,15-octadecatetraenoic acid; *trans*-PnA, *all-trans*-9,11,13,15-octadecatetraenoic acid; PnA, parinaric acid; POPC, 1-palmitoyl-2-oleoyl-*sn*-glycero-3-phosphocholine; $\bar{X}_{chl}$, cholesterol mole fraction; EDTA, ethylenediaminetetraacetic acid; χ^2, mean weighted residue; NMR, nuclear magnetic resonance; $\Delta\sigma_{csa}$, chemical shift anisotropy; Hepes, 4-(2-hydroxyethyl)-1-piperazineethanesulfonic acid.

0006-2960/86/0425-2650$01.50/0

and for the interpretation of residual anisotropy (r_∞) in terms of orientational order parameters (Heyn, 1979; Jähnig, 1979; Lipari & Szabo, 1980; Zannoni et al., 1983).

Materials and Methods

Chemicals. Bovine heart cardiolipins were purchased from Sigma (St Louis, MO) and kept in ethanol (10 mg·mL^{-1}) under argon atmosphere at −20 °C. DOPC was from Serdary (London, Ontario, Canada). Cholesterol (Serva, Heidelberg, West Germany) was dissolved in ethanol (8 mg·mL^{-1}) and kept at −20 °C. These chemicals were found to be pure on analytical high-pressure liquid chromatography (*n*-hexane/2-propanol/water, 6:8:0.75 v/v/v) and were used as supplied. Solutions of *cis*- and *trans*-parinaric acids (Molecular Probes, Junction City, OR) (1 mg·mL^{-1}) were prepared in ethanol saturated with argon and kept at −20 °C.

Vesicle Preparation and Labeling. Ethanol-injected vesicles were prepared according to Kremer et al. (1977) by injecting 0.1 mL of ethanol containing ≃1 mg of cardiolipin or ≃3 mg of DOPC and the apropriate amount of cholesterol into 3 mL of 5 mM Hepes buffer, pH 7.4, containing 0.2 mM EDTA and 0.144 M NaCl at room temperature. Prior to injection, the buffer was extensively bubbled with argon. Fluorescence labeling was achieved by adding 2–5 μL of probe solution into the injected ethanol volume (probe/lipid molar ratio ≃ 1/200).

Fluorescence Measurements. Steady-state fluorescence anisotropy measurements were performed on a T-format SLM 8000 spectrofluoropolarimeter (Urbana, IL), with 319 nm as excitation wavelength (2-nm bandwidth). Schott filters KV 389 were used to select the fluorescence emission. Details of the measurements have been described elsewhere (Vincent et al., 1982a).

Excited-state lifetime and nanosecond anisotropy decay measurements were performed on a time-correlated single photon counting instrument as already described (Vincent et al., 1985) equipped with a nanosecond excitation source from Edimburgh Instruments (Birch & Imhof, 1981). The flash lamp was run in 1.5 atm of nitrogen and at 30 kHz and 8 kV, with an electrode gap of 0.6 mm. Excitation wavelength was selected at 319 nm by a monochromator (5-nm bandwidth). Emission was collected through a Schott KV 389 cutoff filter. The ratio of stop-to-start pulses reaching the time-to-amplitude converter was kept below 4% to avoid pulse pileup problems. No significant pulses were detected when a blank was performed without fluorophore (absence of scatter). In order to avoid color effect of the phototube, the apparatus response function was obtained after cumulation during the same time of the fluorescence decay of a short lifetime standard (*p*-terphenyl in cyclohexane, τ = 0.95 ns; Berlman, 1971), according to Wahl et al. (1974).

Analysis of the data was performed according to previously described methods (Vincent & Gallay, 1984). Data were interpreted according to the distribution function theory (Lipari & Szabo, 1980; Heyn, 1979; Jähnig, 1979).

^{31}P NMR Spectroscopy. Proton-noise-decoupled ^{31}P NMR spectra were obtained on a Brucker AM 400 NMR spectrometer operating at 162 MHz. A sample of 25 mg of cardiolipin with or without cholesterol (13 mg, i.e., $\bar{X}_{chl}$ = 0.67) was evaporated to dryness under a stream of nitrogen, followed by extensive removal of the solvent under pump vacuum overnight. The dry lipid film was hydrated with 5 mM Hepes buffer, pH 7.4, containing 0.2 mM EDTA and 0.144 M NaCl, followed by extensive vortexing. Spectra were cumulated from up to 10000 transients by employing a 45° pulse (11 μs) and 25-kHz sweep width. A line broadening of 50 Hz was applied to the free induction decay.

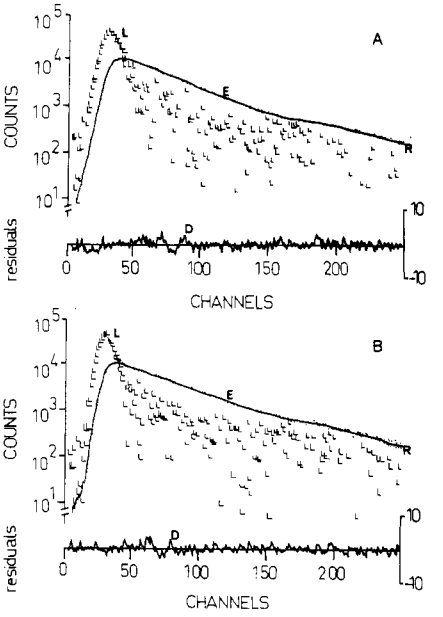

FIGURE 1: (A) Total fluorescence emission decay kinetics of *trans*-parinaric acid in cardiolipin vesicles: excitation wavelength, 319 nm (5-nm bandwidth); "magic angle" configuration (vertical excitation polarizer and emission polarizer orientated 55° from the vertical) (Spencer & Weber, 1970); time resolution, 0.100 ns per channel; temperature, 20 °C. Symbols: L (L), calculated apparatus response function; E (···), experimental curve; R (—), reconvolved curve; D, deviation function. Decay parameters of the best fit: τ_1 = 6.48 ns, a_1 = 0.13, τ_2 = 2.90 ns, a_2 = 0.87, χ^2 = 1.43. (B) Total fluorescence emission decay kinetics of *trans*-parinaric acid in DOPC vesicles: excitation wavelength, 319 nm (5-nm band width); magic angle configuration; time resolution, 0.100 ns per channel; temperature, 20 °C. Decay parameters of the best fit: τ_1 = 5.04 ns, a_1 = 0.47, τ_2 = 2.53, a_2 = 0.53, χ^2 = 1.17.

Results

Total Fluorescence Intensity Decays of cis- and trans-PnA in Cardiolipin Vesicles. Effect of Cholesterol and Comparison with DOPC Vesicles. In cardiolipin vesicles, the *cis*- and *trans*-PnA probes do not exhibit monoexponential fluorescence decay laws. A satisfactory fit is provided by biexponential models as revealed by the low χ^2 values obtained and by the deviation function (Grinvald & Steinberg, 1974), as exemplified on Figure 1 for *trans*-PnA. This situation has been encountered in other lipid species either in the gel or in the liquid-crystalline phase (Wolber & Hudson, 1981). In cardiolipin vesicles, the amplitudes of each lifetime component were almost equal for *cis*-PnA whereas for the trans isomer ≃90% of the emission was resulting from the short lifetime component. This last result is quite different from the one obtained in the DOPC liquid-crystalline phase, where for *trans*-PnA, both lifetime components contribute almost equally to the total emission (Figure 1). It should be observed that in a pure organic solvent such as butanol, a single exponential decay is observed for *cis*-PnA (τ = 2.68 ns, χ^2 = 1.35 at 20 °C). For *trans*-PnA, a minute contribution of a long lifetime component was detected (τ_1 = 1.42 ns, a_1 = 0.997, τ_2 = 6.51 ns, a_2 = 0.003, χ^2 = 1.27).

Upon cholesterol incorporation into cardiolipin vesicles, the total intensity decay parameters are strongly affected for both probes (Figure 2). However, this effect is observed only above a sterol mole fraction ($\bar{X}_{chl}$) of ≃0.20, whereupon the values of the lifetime components and of their amplitudes are strongly enhanced. The effect on the amplitude is more important for *trans*-PnA than for *cis*-PnA (Figure 2). For comparison, similar measurements were performed in the liquid-crystalline phase of DOPC. As in cardiolipin vesicles, cholesterol in-

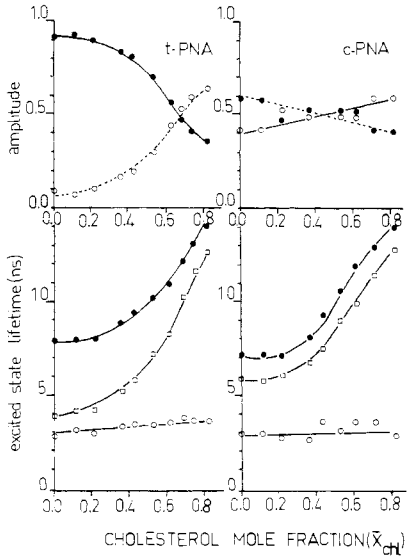

FIGURE 2: Variation of the total intensity decay parameters of parinaric acids in cardiolipin vesicles as a function of the cholesterol mole fraction: (□) mean excited-state lifetime calculated as $\langle\tau\rangle = \sum_i a_i\tau_i^2/\sum_i a_i\tau_i$ (Ross et al., 1981); first (●) and second (○) component parameters.

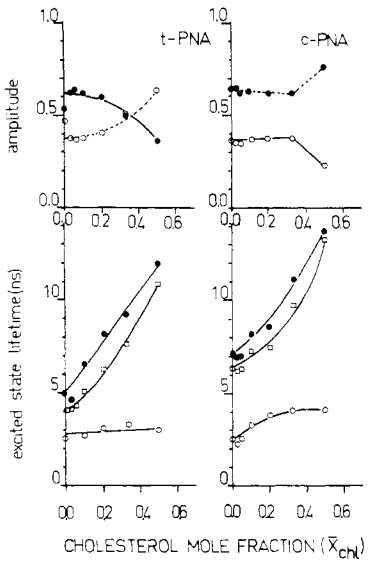

FIGURE 3: Variation of the total intensity decay parameters of *cis*- and *trans*-parinaric acids in DOPC vesicles as a function of the cholesterol mole fraction: (□) mean excited-state lifetime $\langle\tau\rangle$ as defined in the legend of Figure 2; first (●) and second (○) component parameters.

corporation enhanced the mean excited-state lifetime value. This results primarily from the contribution of the long lifetime component (Figure 3). However, in DOPC, the variation of the mean excited-state lifetime as a function of $\bar{X}_{chl}$ differs in two main aspects from that in cardiolipins. First, no latency can be observed at a sterol mole fraction lower than 0.15–0.20. Second, the maximum value obtained in cardiolipin vesicles at a $\bar{X}_{chl} = 0.80$ is obtained in DOPC at a much lower sterol mole fraction of 0.50, the limit of solubility of cholesterol in lecithin systems (Demel & de Kruijff, 1976).

Steady-State and Time-Resolved Fluorescence Anisotropy of cis- and trans-PnA in Cardiolipin Vesicles as a Function of Cholesterol Content. Comparison with DOPC Vesicles. Upon incorporation of cholesterol into cardiolipin vesicles the steady-state anisotropy values of the *cis*- and *trans*-PnA probes are strikingly enhanced (Figure 4). As observed for the total intensity decay parameters, the effect begins only above a

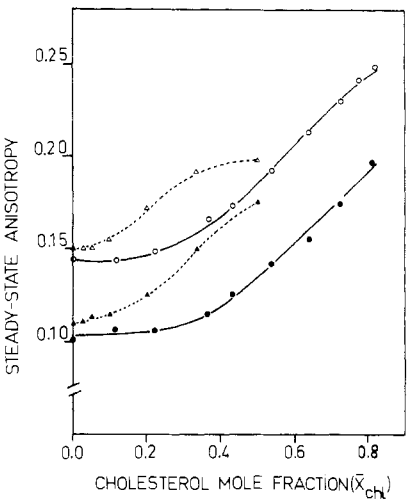

FIGURE 4: Variation of the steady-state anisotropy values of *cis*- and *trans*-parinaric acids in cardiolipin and in DOPC vesicles as a function of the cholesterol mole fraction: *trans*-PnA in (○) cardiolipin and (△) DOPC vesicles; *cis*-PnA in (●) cardiolipin and (▲) DOPC vesicles.

cholesterol mole fraction of ≃0.20. The increase in the anisotropy values is continuous up to the maximum cholesterol mole fraction studied ($\bar{X}_{ch6} \simeq 0.80$). For comparison, the results obtained for DOPC are also presented in Figure 4. No latency can be observed, and the cholesterol effect increases up to $\bar{X}_{chl} = 0.50$, as observed by many techniques in PC or PE systems (Demel & de Kruijff, 1976).

Time-resolved fluorescence anisotropy measurements performed on both lipid systems allow discrimination between the cholesterol effect on the orientational order parameter and (or) on the wobbling motion of the probes in the lipid matrix. Two models were tried to fit the experimental curves, either a sum of two exponentials

$$r(t) = r_{t=0}[a \exp(-t/\Phi_1) + (1 - a) \exp(-t/\Phi_2)] \quad (1)$$

or an exponential function plus a constant

$$r(t) = (r_{t=0} - r_\infty) \exp(-t/\Phi) + r_\infty \quad (2)$$

where $r_{t=0}$—taken as a free parameter—is the effective value of the anisotropy at zero time, r_∞ is the nonzero value of the anisotropy at long time after the excitation, and Φ is the apparent correlation time in the restricted volume of rotation (Kinosita et al., 1977; Lipari & Szabo, 1980).

In pure cardiolipin vesicles and in cholesterol–cardiolipin mixed vesicles at low $\bar{X}_{chl}$, the anisotropy decays can be fit by either model on the basis of χ^2 values. At high $\bar{X}_{chl}$, the second model (eq 2) gave an unambiguous fit of the raw data according to the same criteria. For the sake of comparison we have selected an interpretation of the data in terms of restricted motion.

A similar situation was also met with the anthroyloxy fatty acids in the liquid-crystalline phase of saturated and unsaturated lecithins (Vincent et al., 1982a,b; Vincent & Gallay, 1984). Typical anisotropy decay curves are represented for *cis*-PnA in Figure 5. Similar curves were recorded for *trans*-PnA. Both probes experienced similar rotational barriers as reflected from the similar nonzero values of the anisotropy at long time after the excitation pulse (r_∞) (Figure 6), in the cardiolipin liquid-crystalline phase. The apparent correlation time values were also similar ($\Phi \simeq 2$ ns). Incorporation of cholesterol does not induce any significant change in the r_∞ value up to a sterol mole fraction of 0.20 for both probes (Figure 6). Above this mole fraction, r_∞ increases more sharply for the trans isomer than for the cis one and reaches very high values for $\bar{X}_{chl} \simeq 0.80$.

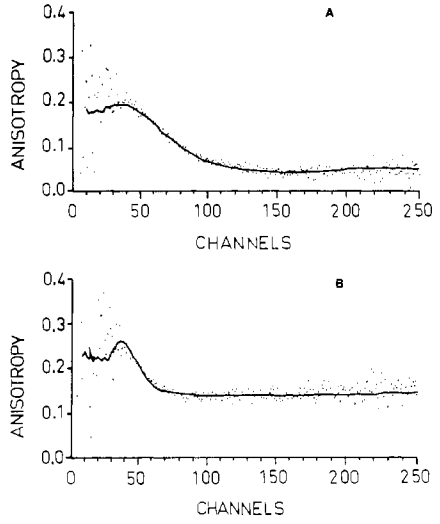

FIGURE 5: Fluorescence anisotropy decay of *cis*-parinaric acid in cardiolipin vesicles. The decay curves were fitted to the following function: $r(t) = (r_{t=0} - r_\infty) \exp(-t/\Phi) + r_\infty$, where $r_{t=0}$ is the anisotropy at zero time, r_∞ the residual anisotropy, and Φ the apparent correlation time. (A) No cholesterol present. Time resolution: 0.100 ns per channel. Decay parameters: $\Phi = 1.64$ ns, $r_{t=0} = 0.239$, $r_\infty = 0.035$. (B) $\bar{X}_{chl} = 0.67$. Time resolution: 0.200 ns per channel. Decay parameters: $\Phi = 0.95$ ns, $r_{t=0} = 0.315$, $r_\infty = 0.140$.

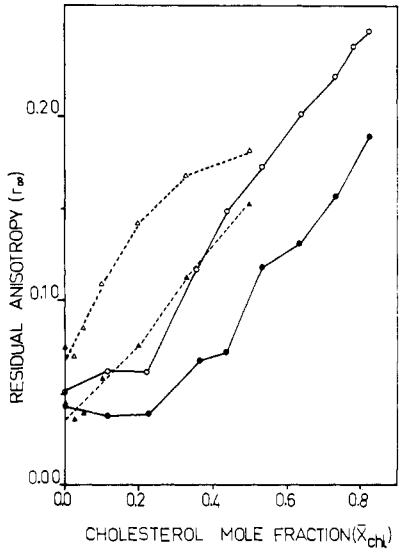

FIGURE 6: Variation of the residual fluorescence anisotropy (r_∞) of *cis*- and *trans*-parinaric acids in cardiolipin and in DOPC vesicles as a function of the cholesterol mole fraction: *trans*-PnA in (○) cardiolipin and (△) DOPC vesicles; *cis*-PnA in (●) cardiolipin and (▲) DOPC vesicles.

A quite different situation is observed in the DOPC liquid-crystalline phase as a function of $\bar{X}_{chl}$ (Figure 6). First, as for the other fluorescence parameters of PnA's, no latency is observed, and second, the increase in r_∞ values levels off for $\bar{X}_{chl} = 0.50$. In addition, *trans*-PnA exhibits a higher r_∞ value of pure DOPC than in pure cardiolipins.

The average orientational order parameter (S) of *cis*- and *trans*-PnA in both lipid systems calculated from r_∞ values according to Lipari and Szabo (1980) exhibits very high values in cardiolipin vesicles upon incorporation of high cholesterol levels (Table I).

^{31}P NMR Spectroscopy of Cardiolipin Vesicles. Even at the highest cholesterol mole fraction in cardiolipin vesicles no aggregation or precipitation could be observed. ^{31}P NMR spectra of multilamellar liposomes evidence neither a "hexagonal" type line shape nor an "isotropic" peak, suggesting

Table I: Average Orientational Order Parameter (S) of *cis*- and *trans*-PnA in Cardiolipin Vesicles as a Function of the Mole Fraction of Cholesterol[a]

	$\bar{X}_{chl}$			
	0	0.23	0.54	0.78
cis-PnA	0.332	0.316	0.549	0.634
trans-PnA	0.357	0.398	0.665	0.780

[a] S values were calculated according to the expression $S = (r_\infty/r_0)^{1/2}$ (Heyn, 1979; Jähnig, 1979; Lipari & Szabo, 1980), taking $r_0 = 0.391$ (Jameson et al., 1978).

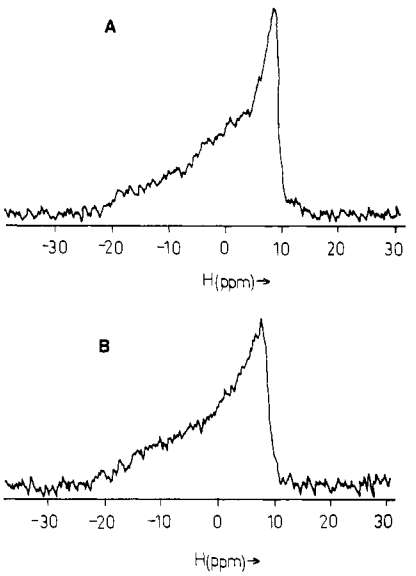

FIGURE 7: ^{31}P NMR spectra (162 MHz) of a dispersion of (A) pure cardiolipin and (B) a cholesterol–cardiolipin mixture ($\bar{X}_{chl} = 0.67$).

that the host phospholipid is still organized in lamellar phase (Figure 7). The anisotropy parameter $\Delta\sigma_{csa}$ has a value of about 32 ppm as recently reported (Powell & Marsh, 1985) and is slightly decreased upon cholesterol incorporation as in PC and PE systems (Brown & Seelig, 1978).

Discussion

Cardiolipins are characteristic phospholipids present in mitochondrial inner membranes and in some bacteria (Ioannou & Golding, 1979). This peculiar phospholipid may be essential for the activity of some mitochondrial enzymes, for instance, cytochrome oxidase (Vik et al., 1981; Robinson, 1982), the mitochondrial phosphate carrier (Cheneval et al., 1983), and cytochrome P-450$_{scc}$, responsible for the side chain cleavage of cholesterol in the steroidogenic tissues (Lambeth, 1981; Pember et al., 1983). In the latter system, it has been shown that the affinity of cholesterol for the cytochrome was much higher when, instead of lecithins, cardiolipin recombinants were used. This last observation raises the question of whether the modification of cholesterol binding to specialized cardiolipin-dependent proteins by this peculiar phospholipid could be explained by cholesterol–cardiolipin interactions weaker than cholesterol–lecithin interactions. The existence of such weak interactions would also provide a partial explanation for the relatively low level of cholesterol in cardiolipin-rich membranes.

These interactions were studied by fluorescence techniques including steady-state and time-resolved fluorescence anisotropy measurements as well as excited-state lifetime measurements. *cis*- and *trans*-parinaric acids are well suited for such studies since they exert a minimal perturbation on their microenvironment (Sklar et al., 1975). Another interesting property of these probes resides in their differential partitioning

between liquid and solid phases (Sklar et al., 1979a,b; Welti, 1982; Welti & Silbert, 1982). Due to its preferential association with solid phase and enhanced quantum yield in phospholipid solid phase, *trans*-PnA has been claimed to be $\simeq$25 times more sensitive to this phase (Sklar et al., 1979a). In contrast, it has been difficult to detect lateral phase separations with *cis*-PnA in phospholipid mixtures. However, the interpretation of the characteristics of the fluorescence emission kinetics of PnA's in terms of differential partitioning inside the lipid bilayer has been recently questioned, considering the multiexponential decays found for these probes in pure isotropic solvents by multifrequency phase fluorometry (Parassassi et al., 1984). Nonexponential decay laws are found in many instances and have been widely discussed in recent reports (DeToma et al., 1976; Lakowicz & Cherek, 1980; Ross et al., 1981). As a prerequisite to explain the different behaviors of PnA's in phospholipid membranes in terms of heterogeneity, these probes must exhibit similar excited-state properties and rotational dynamics in isotropic, homogeneous solvents. In this respect, as pointed out by Wolber and Hudson (1981), a solvent in which formation of micelles is highly unlikely to occur must be chosen. In alcoholic solutions, chosen to discourage monomer association and inverse micelle formation, monoexponential decays for the total fluorescence emission of *cis*-PnA were found, in agreement with the results reported by Wolber and Hudson (1981). For *trans*-PnA, addition of a long time component improved the fit (in terms of the χ^2 value), but the contribution of the preexponential factor associated with this long time component was very small (<0.3%). Moreover, in alcoholic solutions, the rotational dynamics of these probes appeared to be very similar (Wolber & Hudson, 1981). These observations led us to consider the behavior of these probes in membranes partially reflecting membrane inhomogeneity. Indeed, in membrane systems, heterogeneity of environment and the existence of rotational barriers would lead to nonexponential decay laws (Wahl, 1975). A distribution of excited-state lifetimes is likely to occur which may differ for each PnA isomer depending upon (i) their environment and (ii) their excited-state properties. By combining total fluorescence intensity and anisotropy decay measurements, one can obtain a better description of the differential partitioning of these probes.

Acyl Chain Order and Dynamics of Pure Cardiolipin and Pure DOPC Vesicles in the Liquid-Crystalline Phase. In both lipid systems, the steady-state anisotropy values were higher for *trans*-PnA than for *cis*-PnA. In cardiolipin vesicles, this result can be attributed to the existence of a mean excited-state lifetime shorter for the trans than for the cis probe, 90% of the emission of the former probe arising from the short lifetime component. This would indicate (Sklar et al., 1979a; Wolber & Hudson, 1981) that *trans*-PnA did not detect large amounts of solid region in the cardiolipin liquid-crystalline phase. In agreement with this remark was the observation that the r_∞ values were the same for both PnA isomers as were also the apparent correlation time values. Therefore, both probes sensed the same fluid microenvironment in cardiolipin liquid-crystalline phase. There is a quite different situation in DOPC since r_∞ values were higher for *trans*-PnA than for *cis*-PnA. This indicates that, even at the high reduced temperature at which the measurements were performed, some solid regions were sensed by *trans*-PnA in DOPC, a result in agreement with the higher value of the long lifetime amplitude found in this last system for *trans*-PnA as compared to cardiolipin. A persistence of order above the transition temperature has been previously detected in unsaturated PC's (Lee et al., 1974; Wu & McConnell, 1975). More recently, with the *n*-(9-anthroyloxy) fatty acid probes, a persistence of order was also detected above the transition temperature of POPC, and especially in the CH_2 region near the polar head group (Vincent & Gallay, 1984).

Acyl Chain Order and Dynamics of Cholesterol–Cardiolipin and Cholesterol–DOPC Vesicles. Cholesterol incorporation into cardiolipin vesicles was accompanied by severe restrictions of the acyl chain motion as revealed by the variations of the average orientational order parameter of *cis*- and *trans*-PnA probes, the latter one appearing to be the most sensitive to this effect. This can be explained according to the above-mentioned concept that *trans*-PnA sensed preferentially the immobilized region, i.e., in this case in the neighborhood of the cholesterol molecules, whereas the cis isomer did not show any preference for the solid or fluid region (Sklar et al., 1977b, 1979a,b; Wolber & Hudson, 1981). Addition of cholesterol did not affect the short lifetime value of *trans*-PnA to a large extent but only its relative amplitude. This indicates that, as a function of cholesterol content, the amount of the fluid phase decreased but was still present at the highest sterol mole fractions. A similar situation was also observed in DOPC. That cholesterol does not form a homogeneous mixture in PC systems in the liquid-crystalline phase has been suggested (Rubenstein et al., 1979; Lentz et al., 1980; Recktenwald & McConnell 1981). The present results of total intensity decays suggest that inhomogeneous mixtures may be formed also in cardiolipin–cholesterol mixtures. Such an interpretation is strengthened by the anisotropy decay data. It was clearly observed that the variation of the order parameter (S) was different for each probe; the trans isomer was always more sensitive to cholesterol addition than the cis isomer. However, as already underlined for PC systems (Rubenstein et al., 1980), the heterogeneity of cholesterol–cardiolipin mixtures may not correspond to formation of persistent domains but rather to formation of cholesterol-rich regions slow to disrupt in the fluorescence time scale.

At relatively low mole fractions ($\bar{X}_{chl} < 0.20$), cholesterol did not affect the order and dynamics of the cardiolipin acyl chains. This "latency" was observed for the other dynamic parameters of both PnA isomers. It seems to be a peculiar property of cardiolipin bilayers since in PC systems in the liquid-crystalline phase no such latency could be observed, as demonstrated for DOPC. In that last system, even a cholesterol mole fraction as low as 0.05 produced an effect, especially for the *trans*-PnA probe. One could argue that the presence of large amounts of linoleoyl acyl chains ($\simeq$90%) in bovine heart cardiolipin vesicles would preclude any strong interaction with cholesterol since, in PC monolayer systems, no condensing effect of cholesterol has been observed with dilinoleoylphosphatidylcholine up to a 1:1 cholesterol/phospholipid molar ratio (Demel et al., 1972). However, such an interpretation is difficult to reconcile with the observation of a rigidifying effect up to a molar ratio of 4 cholesterol molecules per cardiolipin. It is noteworthy that cardiolipins, when spread as an oriented monolayer at an air–water interface, displayed a limiting molecular area of $\simeq$110 Å^2 (Shah & Schulman, 1965). This is much higher than the value of $\simeq$78 Å^2 reported for PC's (Demel et al., 1972) and reflects the fact that cardiolipin is a double phospholipid. By the way, it could accommodate more cholesterol than PC's on the basis of phospholipid molecules but approximately the same amount on the basis of fatty acyl chain number. Nevertheless, it remains that the major difference between PC, PE, and CL resides in the latency range of cholesterol mole fractions below

$\bar{X}_{chl} \simeq 0.20$ where no ordering effect was detected in cardiolipin–cholesterol mixed vesicles. These data can be interpreted in terms of repulsive interactions between the cardiolipin head groups, which would allow enough space for few cholesterol molecules to be accommodated without disturbing the acyl chain ordering to a large extent.

In conclusion, the observation that cardiolipin membranes are able to accommodate large amounts of cholesterol is in line with the fact that inner mitochondrial membranes, in which cardiolipins are a major phospholipid component, have been shown to be able to incorporate much higher amounts of cholesterol than the physiological resting level (Madden et al., 1980; de Paillerets et al., 1984). This phenomenon is of crucial importance in specialized tissues like the steroidogenic glands which utilize cholesterol as a precursor for steroid hormone biosynthesis. On the other hand, the absence of a cholesterol rigidifying effect at low sterol mole fraction in pure cardiolipin vesicles is indicative of sterol–cardiolipin interactions weaker than with PC systems. These weaker interactions can allow a facilitated exchange of cholesterol molecules between the inner mitochondrial membranes and the cytosolic transport proteins and can provide a partial explanation for the relatively low cholesterol level in these cardiolipin-rich membranes.

ACKNOWLEDGMENTS

We are indebted to Dr. Lhoste and to Dr. Dimicoli for helping us in the ^{31}P NMR measurements on the spectrometer of their laboratory (INSERM U.219). We thank Dr. E. Dufourc (CNRS, Talence, Bordeaux) for helpful advice, as well as Cathy Royer for careful correction of the English. We also thank F. Gonzales for typing the manuscript.

Registry No. CHL, 57-88-5; DOPC, 4235-95-4.

REFERENCES

Berlman, I. B. (1971) *Handbook of Fluorescence Spectra of Aromatic Molecules*, 2nd ed., Academic Press, New York and London.

Birch, D. J. S., & Imhof, R. E. (1981) *Rev. Sci. Instrum. 52*, 1206–1212.

Blume, A., & Griffin, R. G. (1982) *Biochemistry 21*, 6230–6242.

Boggs, J. M., & Hsia, J. C. (1973) *Can. J. Biochem. 51*, 1451–1459.

Brown, M. F., & Seelig, J. (1978) *Biochemistry 17*, 381–384.

Brückdorfer, K. R., & Graham, J. G. (1976) in *Biological Membranes* (Chapman, D., & Wallach, D. F. H., Eds.) Vol. 3, pp 103–152, Academic Press, London.

Chanderbahn, R., Noland, B. J., Scallen, T. J., & Vahouny, G. V. (1982) *J. Biol. Chem. 257*, 8928–8934.

Cheneval, D., Müller, M., & Carafoli, E. (1983) *FEBS Lett. 159*, 123–126.

Cullis, P. F., Van Dijck, P. W. M., De Kruijff, B., & De Gier, J. (1978) *Biochim. Biophys. Acta 513*, 21–30.

Demel, R. A., & de Kruijff, B. (1976) *Biochim. Biophys. Acta 457*, 109–132.

Demel, R. A., Geurts Van Kessel, W. S. M., & Van Deenen, L. L. M. (1972) *Biochim. Biophys. Acta 266*, 26–40.

Demel, R. A., Jansen, J. W. C. M., Van Dijck, P. W. M., & Van Deenen, L. L. M. (1977) *Biochim. Biophys. Acta 465*, 1–10.

De Paillerets, C., Gallay, J., & Alfsen, A. (1984) *Biochim. Biophys. Acta 772*, 183–191.

DeToma, R. P., Easter, J. H., & Brand, L. (1976) *J. Am. Chem. Soc. 98*, 5001–5007.

Ghosh, R., & Seelig, J. (1982) *Biochim. Biophys. Acta 691*, 151–160.

Grinvald, A., & Steinberg, I. Z. (1974) *Anal. Biochem. 59*, 583–588.

Heyn, M. (1979) *FEBS Lett. 108*, 359–364.

Ioannou, P. V., & Golding, B. T. (1979) *Prog. Lipid Res. 17*, 279–318.

Jähnig, F. (1979) *Proc. Natl. Acad. Sci. U.S.A. 76*, 6361–6365.

Jameson, D. M., Weber, G., Spencer, R. D., & Mitchell, G. (1978) *Rev. Sci. Instrum. 49*, 510–514.

Kinosita, K., Kawato, S., & Ikegami, A. (1977) *Biophys. J. 20*, 289–305.

Kremer, J. M. H., Esker, M. W., Pathmamanoharan, C., & Wiersema, P. H. (1977) *Biochemistry 16*, 3932–3935.

Lakowicz, J. R., & Cherek, H. (1980) *J. Biol. Chem. 255*, 831–834.

Lambeth, J. D. (1981) *J. Biol. Chem. 256*, 4757–4762.

Lange, Y., & d'Alessandro, J. S. (1977) *Biochemistry 16*, 4339–4343.

Lange, Y., & Matthies, H. J. G. (1984) *J. Biol. Chem. 259*, 14624–14630.

Lee, A. G., Birdsall, N. J. M., Metcalfe, J. C., Toon, P. A., & Warren, G. B. (1974) *Biochemistry 13*, 3699–3705.

Lentz, B. R., Barrow, D. A., & Hoechli, M. (1980) *Biochemistry 19*, 1943–1954.

Lipari, G., & Szabo, A. (1980) *Biophys. J. 30*, 489–506.

Madden, T. D., Vigo, C., Brückdorfer, K. R., & Chapman, D. (1980) *Biochim. Biophys. Acta 599*, 528–537.

Parassassi, T., Conti, F., & Gratton, E. (1984) *Biochemistry 23*, 5660–5664.

Pember, S. O., Powell, G. L., & Lambeth, J. D. (1983) *J. Biol. Chem. 258*, 3198–3206.

Powell, G. L., & Marsh, D. (1985) *Biochemistry 24*, 2902–2908.

Pugh, E. L., Kates, M., & Szabo, A. G. (1982) *Chem. Phys. Lipids 30*, 55–69.

Recktenwald, D. J., & McConnell, H. M. (1981) *Biochemistry 20*, 4505–4510.

Robinson, N. C. (1982) *Biochemistry 21*, 41–47.

Ross, J. B. A., Rousslang, K. W., & Brand, L. (1981) *Biochemistry 20*, 4361–4369.

Rouser, G. (1983) in *Membrane Fluidity in Biology* (Aloia, R. C., Ed.) Chapter 7, pp 236–289, Academic Press, New York.

Rubenstein, J. L. R., Smith, B. A., & McConnell, H. M. (1979) *Proc. Natl. Acad. Sci. U.S.A. 76*, 15–18.

Rubenstein, J. L. R., Owicki, J. C., & McConnell, H. M. (1980) *Biochemistry 19*, 569–573.

Shah, D. O., & Schulman, J. H. (1965) *J. Lipid Res. 6*, 341–346.

Sklar, L. A., Hudson, B. S., & Simoni, R. D. (1975) *Proc. Natl. Acad. Sci. U.S.A. 72*, 1649–1653.

Sklar, L. A., Hudson, B. S., Petersen, M., & Diamond, J. (1977a) *Biochemistry 16*, 813–819.

Sklar, L. A., Hudson, B. S., & Simoni, R. D. (1977b) *Biochemistry 16*, 819–828.

Sklar, L. A., Miljanich, G. P., & Dratz, E. A. (1979a) *Biochemistry 18*, 1707–1716.

Sklar, L. A., Miljanich, G. P., Burstein, S. L., & Dratz, E. A. (1979b) *J. Biol. Chem. 254*, 9583–9591.

Spencer, R. D., & Weber, G. (1970) *J. Chem. Phys. 52*, 1654–1663.

Tecoma, E. S., Sklar, L. A., Simoni, R. D., & Hudson, B. S. (1977) *Biochemistry 16*, 829–835.

Van Dijck, P. W. M., De Kruijff, B., Van Deenen, L. L. M., De Gier, J., & Demel, R. A. (1976) *Biochim. Biophys. Acta 455*, 576–587.
Vik, S. B., Gegevitch, G., & Capaldi, R. A. (1981) *Proc. Natl. Acad. Sci. U.S.A. 78*, 1456–1460.
Vincent, M., & Gallay, J. (1984) *Biochemistry 23*, 6514–6522.
Vincent, M., De Foresta, B., Gallay, J., & Alfsen, A. (1982a) *Biochemistry 21*, 708–716.
Vincent, M., De Foresta, B., Gallay, J., & Alfsen, A. (1982b) *Biochem. Biophys. Res. Commun. 107*, 914–921.
Vincent, M., Gallay, J., De Bony, J., & Tocanne, J. F. (1985) *Eur. J. Biochem. 150*, 341–347.
Wahl, Ph. (1975) *Chem. Phys. 7*, 220–226.
Wahl, Ph., Auchet, J. C., & Donzel, B. (1974) *Rev. Sci. Instrum. 45*, 28–32.
Welti, R. (1982) *Biochemistry 21*, 5690–5693.
Welti, R., & Silbert, D. F. (1982) *Biochemistry 21*, 5685–5689.
Wolber, P. K., & Hudson, B. S. (1981) *Biochemistry 20*, 2800–2810.
Wu, S. H. W., & McConnell, H. M. (1975) *Biochemistry 14*, 847–854.
Zannoni, C., Arcioni, A., & Cavatorta, P. (1983) *Chem. Phys. Lipids 32*, 179–250.

Photoreversal-Dependent Release of Thymidine and Thymidine Monophosphate from Pyrimidine Dimer-Containing DNA Excision Fragments Isolated from Ultraviolet-Damaged Human Fibroblasts†

Michael Weinfeld,‡ Norman E. Gentner, Lyle D. Johnson, and Malcolm C. Paterson*,‡
Radiation Biology Branch, Health Sciences Division, Chalk River Nuclear Laboratories, Chalk River, Ontario, Canada K0J 1J0
Received October 11, 1985; Revised Manuscript Received December 9, 1985

ABSTRACT: To elucidate the enzymatic excision-repair process operative on cyclobutane-type pyrimidine photodimers in human dermal fibroblasts, we have examined excised dimer-containing material recovered in the trichloroacetic acid soluble fraction from far-ultraviolet-irradiated (254 nm, 40 J m^{-2}) and incubated (24 h) cell cultures. The excised DNA photoproducts were found in oligonucleotide fragments with an estimated mean chain length of ~3.7 bases. Exposure of these isolated excision fragments, labeled with [^{3}H]thymidine (dT), to a secondary, dimer-photoreversing fluence of far-UV (5.5 kJ m^{-2}) resulted in the release of free dT and thymidine monophosphate (TMP). Photorelease of these two radioactive species was measured by high-performance liquid chromatography, with TMP being detected as the increase in dT following bacterial alkaline phosphatase treatment. These data imply that the photoliberated dT and TMP moieties were attached to the excision fragments solely by the cyclobutane ring of the dimer. No evidence was obtained for the photoliberation of free thymine, thus corroborating a conclusion reached by others that the excision of dimers in human cells is not initiated by scission of an intradimer *N*-glycosyl bond. The sum of the tritium label recovered in dT plus TMP corresponded to approximately 40% of that disappearing from thymine-containing dimers on photoreversal, suggesting that in about 80% of the isolated excision fragments the dimer (i) is located at one end of the oligonucleotide and (ii) contains a break in its internal phosphodiester bond. These findings, coupled with our recent studies on xeroderma pigmentosum complementation group A and D cells [Paterson, M. C., Gentner, N. E., Middlestadt, M. V., & Weinfeld, M. (1984) *J. Cell. Physiol., Suppl. 3*, 45–62], lead us to propose cleavage of the intradimer phosphodiester linkage as the initial reaction in the multistep excision-repair process acting on pyrimidine dimers in the DNA of normal human cells.

Cyclobutyl dimers formed between adjacent intrastrand pyrimidines constitute the major photoproducts induced in the DNA of living cells by UV[1] radiation (Setlow, 1966). Studies of the metabolic fate of these lesions in both prokaryotes and eukaryotes have thus far established two principal processes for their restitution, enzymatic photoreactivation, and nucleotide excision repair. The former appears to be specific for pyrimidine dimers; this process is mediated by a DNA photolyase, an enzyme that binds to a dimer-containing site and, upon absorption of visible light energy, simply reverses in situ the cyclization reaction, thereby regenerating the two constitutive pyrimidines (Sutherland, 1978). Photolyase activity has been detected in a wide variety of organisms ranging from simple bacteria to complex mammals, and the enzyme has been

† This work was supported primarily by Atomic Energy of Canada Limited and the U.S. National Cancer Institute through Contract NO1-CP-21029 (Basic) with the Clinical and Environmental Epidemiology Branches, NCI, Bethesda, MD, and in the latter stages of the study by a postdoctoral fellowship to M.W. and a Heritage Medical Scientist award to M.C.P. from the Alberta Heritage Foundation for Medical Research.
* Address correspondence to this author at the Cross Cancer Institute.
‡ Present address: Molecular Genetics and Carcinogenesis Laboratory, Department of Medicine, Cross Cancer Institute, Edmonton, Alberta, Canada T6G 1Z2.

[1] Abbreviations: BAP, bacterial alkaline phosphatase; C◇C, cyclobutane-type photodimer between cytosine and cytosine; C◇T, cyclobutyl cytosine–thymine photodimer; dT, thymidine; HPLC, high-performance liquid chromatography; OD_{260}, optical density measured at 260 nm; ODS, octadecylsilyl; PBS, phosphate-buffered saline; Py◇T, cyclobutyl pyrimidine (cytosine or thymine)–thymine photodimer; SAX, strong-anion exchange; TCA, trichloroacetic acid; TMP, thymidine monophosphate; Thy, thymine; T◇T, cyclobutyl thymine–thymine photodimer; Tris-HCl, tris(hydroxymethyl)aminomethane hydrochloride; U◇T, cyclobutyl uracil–thymine photodimer; U◇U, cyclobutyl uracil–uracil photodimer; UV, ultraviolet; XP, xeroderma pigmentosum.

0006-2960/86/0425-2656$01.50/0